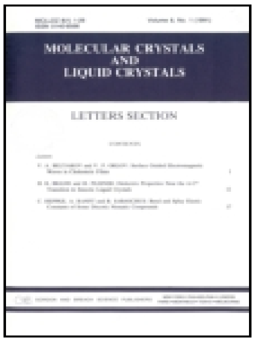

Taylor & Francis
Taylor & Francis Group

Molecular Crystals and Liquid Crystals

ISSN: 1542-1406 (Print) 1563-5287 (Online) Journal homepage: http://www.tandfonline.com/loi/gmcl20

Rheology of Thermotropic Liquid-Crystalline Dendron-Modified Gold Nanoparticles

Masaki Matsubara, Atsushi Miyazaki, Xiangbing Zeng, Atsushi Muramatsu, Goran Ungar & Kiyoshi Kanie

To cite this article: Masaki Matsubara, Atsushi Miyazaki, Xiangbing Zeng, Atsushi Muramatsu, Goran Ungar & Kiyoshi Kanie (2015) Rheology of Thermotropic Liquid-Crystalline Dendron-Modified Gold Nanoparticles, Molecular Crystals and Liquid Crystals, 617:1, 50-57, DOI: 10.1080/15421406.2015.1075818

To link to this article: http://dx.doi.org/10.1080/15421406.2015.1075818

Mol. Cryst. Liq. Cryst., Vol. 617: pp. 50–57, 2015

ISSN: 1542-1406 print/1563-5287 online
DOI: 10.1080/15421406.2015.1075818

Rheology of Thermotropic Liquid-Crystalline Dendron-Modified Gold Nanoparticles

MASAKI MATSUBARA,[1] ATSUSHI MIYAZAKI,[1]
XIANGBING ZENG,[2] ATSUSHI MURAMATSU,[1]
GORAN UNGAR,[2,3] AND KIYOSHI KANIE[1,*]

[1]Institute of Multidisciplinary Research for Advanced Material, Tohoku University, Aoba-ku, Sendai, Japan
[2]Department of Materials Science and Engineering, University of Sheffield, Sheffield, UK
[3]Department of Physics, Zhejiang Sci-Tech University Xiasha College Park, Hangzhou, China

Rheological behavior across thermal phase transitions of liquid crystalline (LC) structures has been investigated using dendron-modified LC gold nanoparticles (NPs) prepared by surface modification of spherical gold NPs with LC dendrons. Such dendron-modified gold NPs self-organize to form a columnar LC structure that transforms to a simple cubic LC structure with increasing temperature. Endo- and exothermic peaks associated with this phase transition are barely observable. However, using dynamic viscoelastic measurements, the transition was observed as a drastic increase in fluidity of the dendron modified gold NPs.

Keywords Liquid Crystal; Rheology; Organic-Inorganic Hybrid Material; Dendrimer; Gold Nanoparticle

1. Introduction

Many attempts to functionalize inorganic nanoparticles (NPs) have been carried out to develop nanostructure-based devices due to their new structure-related functions [1,2]. Well defined NPs have spontaneously formed various kind of self-organized lattices [3–6]. Utilization of mesogenic molecules to modify NPs enables the formation of thermotropic liquid crystalline (LC) phases of NPs [7–14]. Among organic soft materials, organic LC dendrons are the best building blocks to form dendrimer-like spheres by self-assembly. Such spherical assemblies spontaneously form 2- or 3-dimensional self-organized structures [15,16]. Thus, LC dendrons are the most likely candidates to develop NPs-based

---

Present Address of M. Matsubara: Department of Materials and Environmental Engineering, National Institute of Technology, Sendai College, 48 Nodayama, Medeshima-Shiote, Natori 981-1239, Japan

[*] Address correspondence to K. Kanie, Institute of Multidisciplinary Research for Advanced Material, Tohoku University, Katahira 2-1-1, Aoba-ku, Sendai 980-8577, Japan. E-mail: kanie@tagen.tohoku.ac.jp

Color versions of one or more of the figures in the article can be found online at www.tandfonline.com/gmcl.

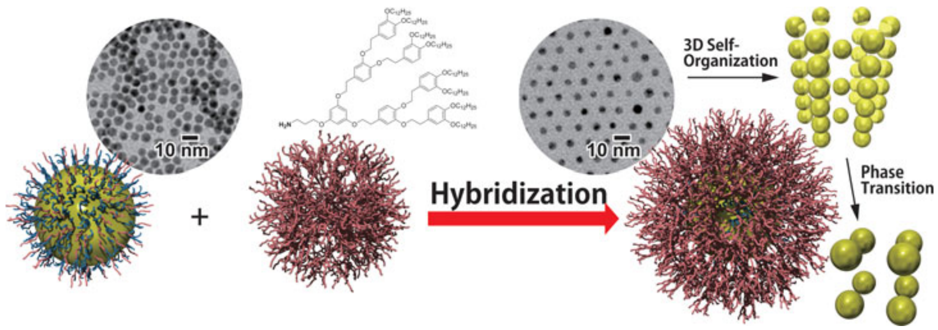

Figure 1. A schematic illustration of dendron-modified gold NPs. The resultant NPs form a 2D hexagonal array on TEM grid and self-organized hexagonal columnar superlattice and a simple cubic LC structure in the bulk.

LC structures. Previously, we have developed the LC dendron-modified gold NPs, which can be regarded as organic-inorganic hybrid dendrimers, with a use of spherical gold NPs as an internal core through surface modification by LC dendrons [17]. The number of organic dendrons attached to the surface of one gold NP can be controlled precisely. The well-defined dendron-modified gold NPs were found to self-organize into a 2D hexagonal LC superlattice and a simple cubic LC phase as shown in Figure 1. Transitions between such phases are often accompanied by endotherms and exotherms. However, differential scanning calorimetry (DSC) experiments on the above systems did not show such peaks. We therefore decided to carry out rheological experiments, since phase transitions are also accompanied by changes in viscoelasticity. So far, many types of phase changes in soft matter have been characterized by rheological analysis, e.g. microphase separations of block copolymers, [18,19] thermotropic LC, [20–23] external stimulus-induced orientation of LC molecules, [24,25] thixotropic gels, and thermal deformations of organogels [26–28]. In the case of organic-inorganic composites, phase transition behavior as well as mechanical properties have also been investigated through rheological analyses [29–35]. For example, the transition from a biphase into a nematic phase of lyotropic LC carbon nanotubes dispersion has been related to the change in viscosity [35]. In this work we focus our attention on rheological analysis of dendron-modified gold NPs [17] to reveal the relationship between the LC structure and its viscoelastic character. The viscoelastic behavior of both dendron molecules and dendron-modified gold NPs have been examined. A drastic decrease in viscosity of the dendron-modified gold NPs has been observed at the thermal LC phase transitions.

2. Experimental

The detailed syntheses of LC dendron **G2**, gold NPs **A2**, and **A3**, **G2**-modified gold NPs **G2/A2**, and **G2/A3** are described in Ref [17]. In the present report, 12-dodecane thiol (DT)-modified gold NPs **A1** was newly synthesized by the method of Zheng et al. [36] with some modifications. Figures 2 and 3 show the chemical structure of **G2** and the TEM images of **A1**-**A3**, respectively. The synthetic procedure for **A1** is as follows: $HAuCl_4 \cdot 4H_2O$ (0.125 mmol) and DT (0.250 mmol) were dissolved into 8.0 mL of THF. The mixed solution was stirred at room temperature for 3 h. Then, the mixture was heated

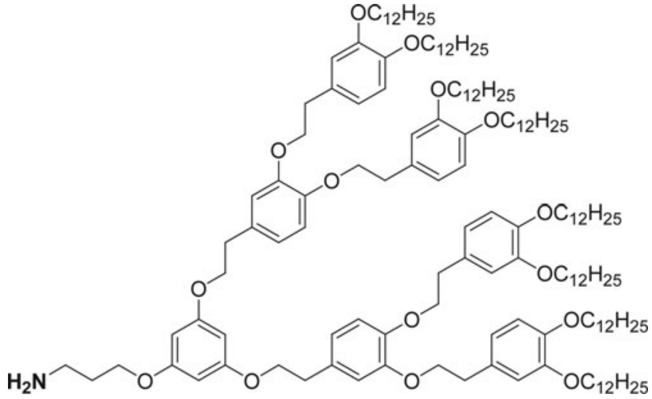

Figure 2. Chemical structure of phenetyl ether-type dendron **G2** used in the present study.

up to 55°C and $BH_3 \cdot t\text{-}BuNH_2$ as reducing agent was added in one portion at the same temperature. The resulting solution was centrifuged, and the precipitate was washed three times with hexane/ethanol. Mercaptohexadecanoic acid (MHA)-modified gold NPs **A2** and **A3** were also prepared in the presence of both DT and MHA as the internal core of **G2**-modified NPs. The initial DT/MHA molar ratio was fixed at 3/2, and 4/1 for the preparation of **A2** and **A3**, respectively, to give different proportions of CO_2H-groups on the surface of NPs. Modification of **A2** and **A3** by **G2** was carried out by amidation reaction between a CO_2H-group and an amino-group to obtain **G2**-modified gold NPs **G2/A2** and **G2/A3**.

Temperature variable dynamic viscoelastic measurements were carried out by using a TA Instruments ARES-G2 Rheometer equipped with 8 mm diameter stainless parallel flat plates. The measurement conditions were: strain 5%, frequency 1.0 Hz, and heating rate 2°C/min.

3. Results and Discussion

SAXS measurements have revealed that **G2** formed a poorly ordered hexagonal columnar phase (Col_h) from room temperature to *ca.* 50°C. After annealing for a long time, **G2** self-assembled into a spherical shape, so that this phase changed to a dodecagonal liquid quasi crystal (LQC) between 60 and 80°C. Further details were reported in Ref [17]. DSC

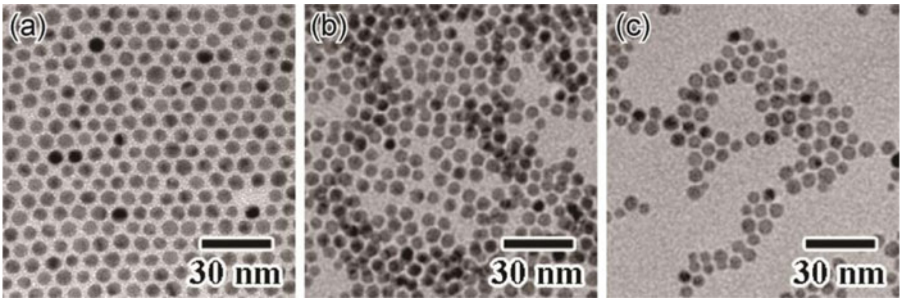

Figure 3. TEM images of hydrophobic DT-modified gold NPs (a) **A1**, and hydrophilic MHA-modified gold NPs (b) **A2**, and (c) **A3**.

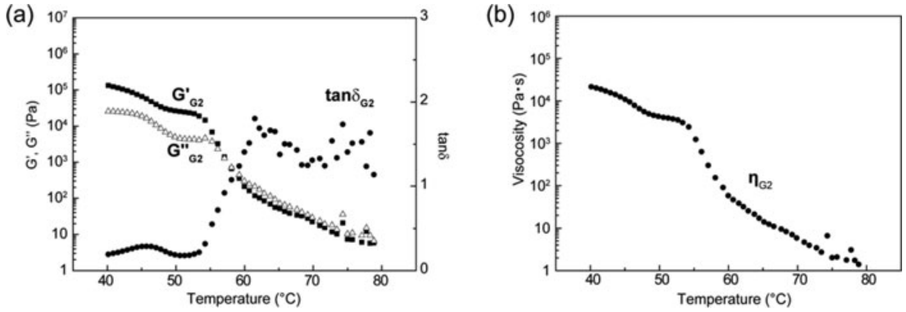

Figure 4. (a) Temperature dependent dynamic viscoelastic curves of **G2**. G′ and G″ are storage and loss moduli, respectively. tanδ (= G″/G′) is the loss tangent. (b) Viscosity of **G2**.

measurements of **G2** showed two endotherms at 14 and 46°C on heating. Figure 4(a) shows temperature variable dynamic viscoelastic curves of **G2**. Here, G′ and G″ denote a storage elastic modulus and a loss elastic modulus, respectively. tanδ = G″/G′ is the loss tangent, which is a measure of energy dissipation. The measurement started from 40°C, where **G2** molecules self-organized in a hexagonal columnar structure with stacking of disk-shaped **G2** assemblies. With increasing temperature, both G′ and G″ of **G2** ($G'_{\mathbf{G2}}$) and ($G''_{\mathbf{G2}}$) decrease. A drastic increase in tan$\delta_{\mathbf{G2}}$ (= $G''_{\mathbf{G2}}/G'_{\mathbf{G2}}$) at 46°C is observed. Such change in tan$\delta_{\mathbf{G2}}$ is due to thermal motions of alkyl chains with increasing temperature. At the same temperature, an endotherm was clearly observed in the DSC scan. According to small-angle X-ray scattering (SAXS), the structure of **G2** both below and above 46°C is Col$_h$. This suggests that a phase transition from an ordered to a disordered Col$_h$ might be occurring by way of glass transition, resulting in an increase in tan$\delta_{\mathbf{G2}}$. As the temperature was further increased to 55°C, tan$\delta_{\mathbf{G2}}$ continued the drastic increase, and exceeded 1.0. This means that **G2** behaved like a liquid, allowing **G2** molecules to self-assemble into spherical shape to form the LQC phase. Such increase in fluidity of **G2** was also confirmed by the observed decrease in viscosity ($\eta_{\mathbf{G2}}$) at 55°C (Figure 4 (b)). Both in the SAXS and DSC measurements, it was difficult to assign a critical phase transition temperature into LQC because it took for a long time to form a thermally stable LQC structure. Actually, an endotherm peak at 55°C was not observed by DSC measurement. However, we could observe the phase transition behavior as the drastic changes in viscosity.

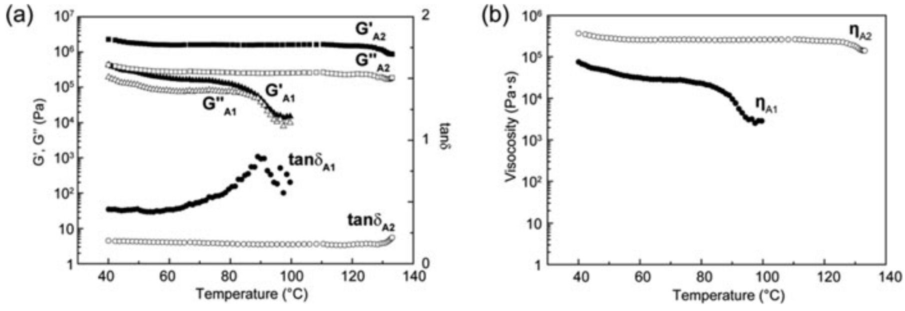

Figure 5. (a) Temperature dependent dynamic viscoelastic curves for **A1** and **A2**. (b) Viscosity of **A1** and **A2**.

Table 1. Diameter of **A1**-**A3** and modification number and ratio of DT and MHA on **A1**-**A3**

	Diameter (nm)	DT/MHA	N_{DT}	N_{MHA}
A1	6.8 ± 0.5	10/0	1310	—
A2	6.8 ± 0.7	10/3.8	600	220
A3	6.8 ± 0.8	10/1.5	680	100

As gold NPs, we have prepared DT-modified gold NPs **A1** and MHA-modified gold NPs **A2** and **A3** as shown in Figure 3. The shapes of the gold cores of **A1**-**A3** were close to spherical with narrow size distributions. The mean size and the distributions of the core parts of **A1**, **A2**, and **A3** were 6.8 ± 0.5, 6.8 ± 0.7, and 6.8 ± 0.8 nm, respectively. From the ^{1}H NMR measurements, methyl-to-carboxylic molar ratios (DT/MHA) on the surface of **A2** and **A3** were determined as 10/3.8 and 10/1.5, respectively (see, Ref [17]). Thermogravimetric (TG) analysis showed that the weight losses of **A1**, **A2**, and **A3** were 12.2, 8.8, and 8.0%, respectively. These losses were attributed to burning off of DT and MHA. The number of DT (N_{DT}) and MHA (N_{MHA}) ligands on a gold NP was calculated and summarized in Table 1 by using the results of ^{1}H NMR and TGA measurements.

Figure 5 (a) shows dynamic viscoelasticity of **A1** and **A2**. In the case of **A1**, a steep decrease in both G′ and G″ of **A1** ($G'_{\mathbf{A1}}$) and ($G''_{\mathbf{A1}}$) was observed, and tan $\delta_{\mathbf{A1}}$ ($= G''_{\mathbf{A1}}/G'_{\mathbf{A1}}$) became unstable and diverged with increasing the temperature. Such divergence behavior of tan$\delta_{\mathbf{A1}}$ at about 100°C might be derived from a thermal decomposition and detachment of DT on the surface of **A1** because irreversible aggregation of **A1** was observed after the measurement. On the other hand, values of G′ and G″ of **A2** ($G'_{\mathbf{A2}}$) and ($G''_{\mathbf{A2}}$) were almost constant in the temperature range from 40°C to 130°C (Figure 5 (a)). Here, tan$\delta_{\mathbf{A2}}$ ($= G''_{\mathbf{A2}}/G'_{\mathbf{A2}}$) was about 0.2. The result suggested that **A2** had no viscoelastic property and formed only powder-like solid state in this temperature range. Such solid-like behavior of **A2** might be derived from the high viscosity of **A2** ($\eta_{\mathbf{A2}}$) against to the corresponding viscosity of **A1** ($\eta_{\mathbf{A1}}$) (Figure 5 (b)). Furthermore, thermal decomposition and detachment of thiols from the surface were negligible for solid-like **A2**. The result suggests that increase in the fluidity of thiol-modified NPs might enhanced thermal decomposition and detachment of the thiols.

According to our previous study, we have prepared **G2**-modified **A2** and **A3** (**G2/A2**) and (**G2/A3**). From the TG results, **G2**-modification numbers of **G2/A2** and **G2/A3** are

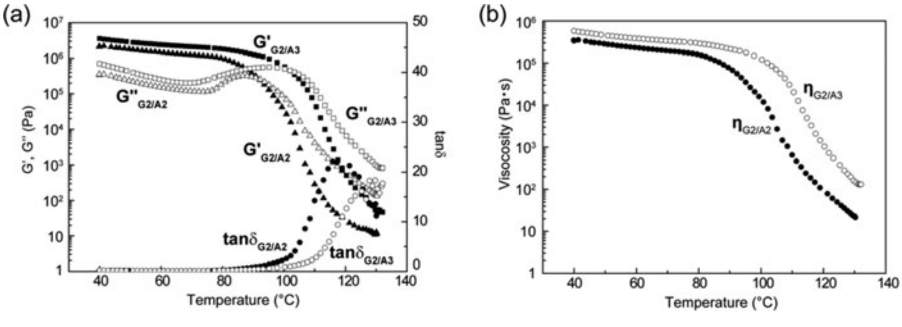

Figure 6. (a) Temperature dependent dynamic viscoelastic curves for **G2/A2** and **G2/A3**. (b) Viscosity of **G2/A2** and **G2/A3**.

calculated as 280 and 80 molecules, respectively (see, Ref [17]). The number of **G2** on **G2/A2** is much higher than that of **G2/A3**. DSC trace for **G2/A2** shows the first endotherm at 9°C a second broad endotherm around 220°C. On the other hand, SAXS measurements reveals that **G2/A2** forms a hexagonal superlattice (HS) LC structure below 130°C, and it exhibits a simple cubic (SC) LC structure at 150°C. However, an endothermic peak derived from phase transition from the HS phase to the SC phase is not observed by the DSC measurement. To catch the phase transition, we focused on rheological analysis. Figure 6 (a) summarizes temperature variable dynamic viscoelastic curves of **G2/A2** and **G2/A3**. Here, G' and G'' of **G2/A2** are plotted as $G'_{\mathbf{G2/A2}}$ and $G''_{\mathbf{G2/A2}}$. Further, G' and G'' of **G2/A3** are also shown as $G'_{\mathbf{G2/A3}}$ and $G''_{\mathbf{G2/A3}}$. Compared with $\tan\delta_{\mathbf{A1}}$, both values of $\tan\delta_{\mathbf{G2/A2}}$ ($= G''_{\mathbf{G2/A2}}/G'_{\mathbf{G2/A2}}$) and $\tan\delta_{\mathbf{G2/A3}}$ ($= G''_{\mathbf{G2/A3}}/G'_{\mathbf{G2/A3}}$) are stable and measurable until *ca.* 120°C. The result suggested that **G2/A2** and **G2/A3** show higher viscoelastic stability than the corresponding DT-modified **A1** NPs. Such increase in the stability might be due to steric repulsion of **G2** on the gold surfaces to prevent aggregation of the gold NPs. In the case of **G2/A2**, $G'_{\mathbf{G2/A2}}$ and $G''_{\mathbf{G2/A2}}$ decreased with increasing in temperature due to thermal motions of alkyl chains of **G2**. The value of $\tan\delta_{\mathbf{G2/A2}}$ exceeded 1.0 at 92°C, so that fluidity increased. As fluidity increased, **G2/A2** formed the LC HS structure. This behavior is similar to **G2** forming the self-organized $\mathrm{Col_h}$ LC structure. Above 120°C, $\tan\delta_{\mathbf{G2/A2}}$ became gradually unstable and diverged. Here, **G2/A2** was thermally stable until *ca.* 170°C, determined by TG-DTA and SAXS measurements. Furthermore, irreversible aggregation, observed in the case for **A1**, was not seen for **G2/A2**. These results suggests divergence behavior observed here is not derived from the decomposition and/or detachment of thiols on the surface of **G2/A2** but derived from drastic decrease in the viscosity. Actually, viscosity of **G2/A2** ($\eta_{\mathbf{G2/A2}}$) rapidly decreased from 3.4×10^5 Pa·s at 40°C to 2.2×10^1 Pa·s at 130°C (Figure 5 (b)). In such low viscosity area, dynamic viscoelastic measurement applying with 5% of strain involves measurement deviation problems. The drastic change in $\eta_{\mathbf{G2/A2}}$ of **G2/A2** on its heating is the most likely cause of the transition from the metastable HS to the stable SC phase. On the other hand, as shown in Figure 6 (a), even though the dynamic viscoelastic behavior of **G2/A3** were similar to those of **G2/A2**, **G2/A3** only forms amorphous-like structure. However, viscosity of **G2/A3** ($\eta_{\mathbf{G2/A3}}$) at 130°C is 1.3×10^2 Pa·s and is 6 times higher than that of **G2/A2**. In order to obtain an ordered structure in **G2/A3**, it may therefore be necessary to anneal the material for longer time and/or at a still higher temperature. This would, however, expose the material to the risk of degradation. Form this point of view, dense surface modification of **G2** on the gold NPs is a most plausible critical role to reduce the viscosity. Furthermore, the present report demonstrated that the large difference in the viscosity might also contribute to introduce LC behavior into NPs.

4. Conclusion

We have investigated the viscoelastic behavior of LC dendron **G2** and **G2**-modified gold NPs **A2** and **A3** by rheological analyses. SAXS and DSC measurements revealed that **G2/A2** forms a hexagonal superlattice LC structure below 130°C, and a simple cubic LC structure at 150°C. However, endotherms (exotherms) corresponding to these phase transitions could not be observed due to their low rate. Dynamic mechanical measurements have demonstrated that these transitions are kinetically controlled, and are triggered by the steep decrease in viscosity associated with the glass transition. Furthermore, the study highlights the importance of lowering the viscosity for the introduction of order into NP systems, and provides a quantitative scale to this already suspected empirical rule. The results shown here should thus help future design and synthesis of NP-based functional materials.

Funding

This work was financially supported by JSPS (Research fellowship for young scientists No. 24 •9313 (MM), Grant-in-aid for young scientific research (A) No. 22685019 (KK), Grant-in-aid for scientific research (B) No. 25288087 (KK), and Bilateral Joint Research Projects (KK)). We acknowledge financial support from the Asahi Glass Foundation (KK) and METI & NEDO Super Hybrid Materials Development Project (AM, KK).

References

[1] Hedayati, M. K., Faupel, F., & Elbahri, M. (2014). *Materials*, *7*, 1221.
[2] Maragò, O. M., Jones, P. H., Gucciardi, P. G., Volpe, G. & Ferrari, A. C. (2013). *Nature Nanotech.*, *8*, 807.
[3] Kiely, C. J., Fink, J., Brust, M., Bethell, D., & Schiffrin, D. J. (1998). *Nature*, *396*, 444.
[4] Shevchenko, E. V., Talapin, D. V., Kotov, N. A., O'Brien, S., & Murray, C. B. (2006). *Nature*, *439*, 55.
[5] Miszta, K., Graaf, J. de, Bertoni, G., Dorfs, D., Brescia, R., Marras, S., Ceseracciu, L., Cingolani, R., Roij, R. van, Dijkstra, M., & Manna, L. ((2011). *Nat. Mater.*, *10*, 872.
[6] Cargnello, M., Diroll, B. T., Gaulding, E. A., & Murray, C. B. (2014). *Adv. Mater.*, *26*, 2419.
[7] Kanie, K., & Muramatsu, A. (2005). *J. Am. Chem. Soc.*, *127*, 11578.
[8] Kanie, K., & Sugimoto, T. (2003). *J. Am. Chem. Soc.*, *125*, 10518.
[9] Mang, X., Zeng, X., Tang, B., Liu, F., Ungar, G., Zhang, R., Cseh, L., & Mehl, G. H. (2005). *J. Mater. Chem.*, *22*, 11101.
[10] Donnio, B., García-Vázquez, P., Gallani, J. L., Guillon, D., & Terazzi, E. (2007). *Adv. Mater.*, *19*, 3534.
[11] Draper, M., Saez, I. M., Cowling, S. J., Gai, P., Heinrich, B., Donnio, B., Guillon, D., & Goodby, J. W. (2011). *Adv. Func. Mater.*, *21*, 1260.
[12] Wojcik, M. M., Gora, M., Mieczkowski, J., Romiszewski, J., Gorecka, E., & Pociecha, D. (2011). *Soft Mater.*, *7*, 10561.
[13] Marx, V. M., Girgis, H., Heiney, P. A., & Hegmann, T. (2008). *J. Mater. Chem.*, *18*, 2983.
[14] Mischler, S., Guerra, S., & Deschenaux, R. (2012). *Chem. Commun.*, *48*, 2183.
[15] Zeng, X., Ungar, G., Liu, Y., Percec, V., Dulcey, A. E., & Hobbs, J. K. (2004). *Nature*, *428*, 157.
[16] Rosen, B. M., Wilson, D. A., Wilson, C. J., Peterca, M., Won, B. C., Huang, C., Lipski, L. R., Zeng, X., Ungar, G., Heiney, P. A., & Percec, V. (2009). *J. Am. Chem. Soc.*, *131*, 17500.
[17] Kanie, K., Matsubara, M., Zeng, X., Liu, F., Ungar, G., Nakamura, H., & Muramatsu, A. (2012). *J. Am. Chem. Soc.*, *134*, 808.
[18] Fredrickson, G. H., & Bates, F. S. (1996). *Annu. Rev. Muter. Sci.*, *26*, 501.
[19] Andreozzi, L., Autiero, C., Faetti, M., Giordano, M., Zulli, F., Galli, G., & Menghetti, S. (2011). *Mol. Cryst. Liq. Cryst.*, *549*, 133.
[20] Mezzenga, R., Meyer, C., Servais, C., Romoscanu, A. I. Sagalowicz, L.,& Hayward, R. C. (2005). *Langmuir*, *21*, 3322.
[21] Pogodina, N. V., Amann, T., Dold, C., Metwalli, E., Müller-Buschbaum, P., Kailer, A., & Friedrich, C. (2014). *J. Mol. Liq.*, *192*, 118.
[22] Fujii, S., Komura, S., & Lu, C.-Y. D. (2014). *Materials*, *7*, 5146.
[23] Yamaguchi, T., Yamada, M., Kutsumizu, S., & Yano, S. (1995). *Chem. Phys. Lett.*, *240*, 105.
[24] Negita, K., & Uchino, S. (2002). *Mol. Cryst. Liq. Cryst.*, *378*, 103.
[25] Pasechnik, S. V., Shmeliova, D. V., Kharlamova, O. A., Chigrinov, V. G., Sun, J., & Dubtsov, A. V. (2012). *Mol. Cryst. Liq. Cryst.*, *560*, 131.
[26] Desbrières, J., Hirrien, M., & Ross-Murphy, S.B. (2000). *Polymer*, *41*, 2451.

[27] Brinksma, J., Feringa, B. L., Kellogg, R. M., Vreeker, R., & Esch, J. van (2000). *Langmuir*, *16*, 9249.

[28] Han, L.-J., Li, L., Zhao, L., Li, B., Liu, G.-Q., Liu, X.-Q., & Wang, X.-D. (2013). *Food Res. Int.*, *53*, 42.

[29] Zhang, Q., & Archer, L. A. (2002). *Langmuir*, *18*, 10435.

[30] Tsenga, W. J., &, Lin, K.-C. (2003). *Mater. Sci. Eng.A*, *355*, 186.

[31] Starr, F. W., Douglas, J. F., & Glotzer, S. C. (2003). *J. Chem. Phys.*, *119*, 1777.

[32] Bhattacharya, S., Srivastava, A., & Pal, A. (2006). *Angew. Chem. Int. Ed.*, *45*, 2934.

[33] Akcora, P., Liu, H., Kumar, S. K., Moll, J., Li, Y., Benicewicz, B. C., Schadler, L.S., Acehan, D., Panagiotopoulos, A. Z., Pryamitsyn, V., Ganesan, V., Ilavsky, J., Thiyagarajan, P., Colby, R. H., & Douglas, J. F. (2009). *Nat. Mater.*, *8*, 354.

[34] Yamamoto, T., Yada, M., & Yokoyama, H. (2004). *Mol. Cryst. Liq. Cryst.*, *409*, 69.

[35] Davis, V. A., Ericson, L. M., Parra-Vasquez, A. N. G., Fan, H., Wang, Y., Prieto, V., Longoria, A. J., Ramesh, S., Saini, R. K., Kittrell, C., Billups, W. E., Adams, W. W., Hauge, R. H., Smalley, R. E., & Pasquali, M. (2004). *Macromolecules*, *37*, 154.

[36] Zheng, N., Fan, J., Stucky, G. D. (2006). *J. Am. Chem. Soc.*, *128*, 6550.